WHITE PAPER

Experimental Evaluation of the Quantum Fourier Transform on a Trapped-Ion Quantum Computer

Mitsui & Co., Ltd.
Quantum Innovation Dept., Corporate Development Div.

Mitsubishi Electric Corporation
Quantum Project Group, Information Technology R&D Center

MITSUI&CO.

MITSUBISHI ELECTRIC
Changes for the Better

Experimental Evaluation of the Quantum Fourier Transform on a Trapped-Ion Quantum Computer

Executive Summary

Abstract

The Quantum Fourier Transform (QFT[Note A1]) is a fundamental quantum operation underpinning a broad range of quantum applications, including cryptanalysis, quantum chemistry, and financial simulation. Because QFT requires many two-qubit operations, it imposes demanding requirements in several respects, including low quantum-gate error rates and high qubit connectivity. In this paper, Mitsui & Co., Ltd. and Mitsubishi Electric Corporation conduct an experimental evaluation of QFT on physical and logical qubits[Note A2] using Quantinuum's trapped-ion quantum computer, Helios®.

On physical qubits, we executed Approximate QFT[Note A1] on the Helios system using 98 physical qubits, **one of the largest scales**[Note A3] for such an evaluation, and evaluated the scaling behavior of the target-state probability P_{target}[Note A4]. On logical qubits, we evaluated QFT with **up to 12 logical qubits** encoded in the Steane code[Note A5], comparing the effects of error-detection post-selection and error correction. Under the conditions of this evaluation, post-selection achieved a logical target-state probability $P^{\text{L}}_{\text{target}}$[Note A4] comparable to or higher than that of error correction. We also compared multiple implementations of the logical T gate[Note A6] on the Helios system.

This evaluation observed a nonzero P_{target} even at 98 physical qubits, while also indicating that continued scaling with physical qubits alone is limited by unavoidable error accumulation. In the logical-qubit evaluation, error-detection post-selection improved $P^{\text{L}}_{\text{target}}$[Note A4], but reduced the acceptance rate[Note A7], revealing a trade-off. Toward the incremental realization of FTQC, implementation design must optimize the balance among P_{target}, $P^{\text{L}}_{\text{target}}$, and acceptance rate according to the computational objective. This calls for an integrated approach spanning the truncation depth of small-angle controlled-phase rotation gates at the algorithm layer, code selection at the error-correction layer, and all-to-all connectivity among qubits.

ABSTRACT NOTES

[Note A1] **QFT / Approximate QFT**: QFT, or the Quantum Fourier Transform, is the quantum analog of the classical discrete Fourier transform and a foundational operation used in many quantum algorithms, including Shor's algorithm. Approximate QFT is an approximate implementation that omits part of the small-angle controlled-phase rotations in the QFT circuit. [Note A2] **Physical / logical qubits**: A physical qubit is a qubit that is directly operated on a quantum computer. A logical qubit is encoded using multiple physical qubits through a quantum error-correction code. [Note A3] **one of the largest scales**: Based on publicly available information as of March 2026, this refers to publicly disclosed evaluations in which Approximate QFT was executed on physical qubits and a nonzero target-state probability was obtained for the output expected from the ideal circuit. [Note A4] **Target-state probability**: P_{target} denotes the probability that the target output expected from the ideal circuit is observed in measurements on the quantum computer. On logical qubits, $P^{\text{L}}_{\text{target}}$ denotes the probability that the target output expected from the ideal logical circuit is observed after decoding or extraction. [Note A5] **Steane code**: A representative quantum error-correction code that encodes one logical qubit using seven physical qubits. [Note A6] **Logical T gate**: A gate on logical qubits that is required, in addition to the basic Clifford gate set, to enable universal quantum computation. It is costly to implement in fault-tolerant quantum computing. [Note A7] **Acceptance rate**: The fraction of trials judged to be valid after error detection and post-selection.

Background

In recent years, quantum resource estimates for cryptanalysis—including attacks on elliptic curve cryptography—have been revised downward, lending greater concreteness to discussions of "Q-Day," the day on which quantum computers will be capable of breaking today's public-key cryptography [1].

The Quantum Fourier Transform (QFT) is a foundational operation used in quantum algorithms across many fields. Understanding how large a QFT circuit can be implemented on today's quantum computers, and whether the target output can still be observed, is an important step toward FTQC.

Progression — From NISQ to FTQC

This evaluation is positioned as an experimental evaluation in the Partial-FTQC phase, where error correction is introduced in part.

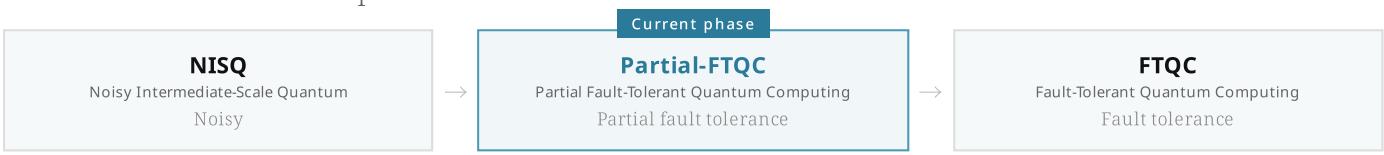

Figure S1. Progression from NISQ to FTQC

Highlights

HIGHLIGHT 01 — PHYSICAL QUBITS

Evaluation of target-state probability scaling in Approximate QFT on 98 physical qubits

Approximate QFT, which uses many two-qubit operations including small-angle controlled-phase rotations and operations between non-adjacent qubits, was executed on 98 physical qubits to evaluate the scaling behavior of P_{target}.

HIGHLIGHT 02 — LOGICAL QUBITS

Experimental Evaluation of error detection, error correction, and logical T gates in QFT on logical qubits

QFT with up to 12 logical qubits was executed using the Steane code, and the effects of error-detection post-selection and error correction were compared. Under the conditions of this evaluation, error-detection post-selection showed a $P_{\text{L}_{\text{target}}}$ among accepted shots that was comparable to or higher than that of error correction. A two-logical-qubit QFT was also used to compare the direct analog rotation method and the code-switching injection method for logical T gates.

HIGHLIGHT 03 — TOWARD FTQC

Trade-off between target-state probability and acceptance rate

The results suggest that a more fault-tolerant implementation is not always optimal; method selection should account for the required $P_{\text{L}_{\text{target}}}$, computational resources, and acceptance rate.

QEC — Quantum Error Correction

For quantum error correction, this evaluation used not only Quantinuum's existing pytket® implementation but also an implementation developed by Mitsubishi Electric with Guppy®, with a view toward a future QEC software foundation, and verified its operation on the Helios system. pytket® is a Python library for building, optimizing, and compiling quantum circuits; Guppy® is a quantum programming language for describing quantum-classical hybrid control.

Hardware — Trapped-Ion Quantum Computer

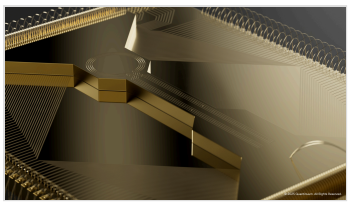

Figure S2. Quantinuum® Helios® Trapped-ion quantum computer

Helios® is a trapped-ion quantum computer commercially released by Quantinuum in November 2025. It uses barium ions as qubits and achieves all-to-all connectivity through a QCCD architecture. It provides 98 physical qubits, with a typical two-qubit gate error rate of approximately 0.08% [2].

Architecture — Quantum-Computer Layer Structure and Key Roles

Key roles in this evaluation: Mitsui & Co. | Mitsubishi Electric

Quantum Applications	**Quantum Applications / Algorithms** — Mitsubishi Electric, Mitsui & Co. **Quantum-computing methods evaluated** Algorithm design, circuit description, and metric design for QFT / Approximate QFT and related methods.
Quantum Algorithms	
Quantum Error Correction	**Quantum Error Correction (Guppy®-based)** — Mitsubishi Electric **QEC foundation toward FTQC** Description and verification of error-detection and error-correction circuits in the Guppy® language.
Quantum Control System	**System Control and Physical Hardware** — Mitsui & Co. **Experimental Environment on the Helios® System** Pulse control, readout, calibration, experimental-sequence implementation, and measurement-data acquisition.
Quantum Processor	

Figure S3. Quantum-computer layer structure, development entities, and responsibilities

Qubits — Physical / Logical Qubits

PHYSICAL QUBIT

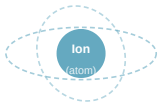

Figure S4. One ion (atom) = one qubit

One ion (atom) corresponds to one qubit. Helios® uses $^{137}Ba^{+}$ ions. Physical qubits are directly affected by physical noise.

LOGICAL QUBIT

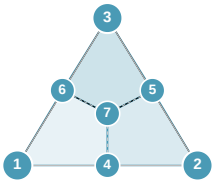

Figure S5. Steane code (7 physical qubits = 1 logical qubit)

In the Steane code, **seven physical qubits (1–7)** encode one logical qubit. The three colored plaquettes correspond to error detection; the code can detect two errors and correct one error.

1. Introduction

1.1 Introduction

Running practical quantum algorithms on a quantum computer requires understanding how stably complex quantum circuits can be executed, how many qubits and how much circuit depth they can reach, and whether the target output can be observed. After encoding into logical qubits, it is also important to determine what target-state probability and acceptance rate can be achieved. Addressing these questions requires a multidimensional evaluation that starts from individual metrics such as gate error rates and qubit count, then considers how they interact.

EVALUATION METRICS

In this paper, we denote the fraction of measurements in which the target output expected from the ideal circuit is observed as the target-state probability P_{target}. For evaluations on logical qubits, we denote the fraction of decoded or extracted measurement results in which the target output expected from the ideal logical circuit is observed as the logical target-state probability $P^{\text{L}}_{\text{target}}$. When post-selection is applied based on detection outcomes, we call the fraction of all shots that remain as valid results the acceptance rate.

1.2 Quantum Fourier Transform (QFT)

The Quantum Fourier Transform (QFT) is a representative quantum operation for extracting phase and periodicity from quantum states. Although it is not itself an end application, it is used as a foundational operation in many applied algorithms, including Quantum Phase Estimation (QPE) and Shor's algorithm (see Figure 1).

Figure 1. Positioning of QFT / Approximate QFT

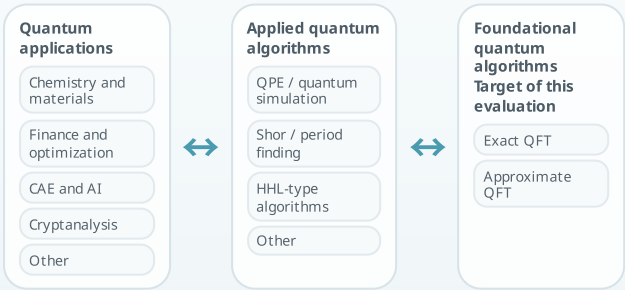

Examining how far QFT can be executed on the Helios system, and whether the target output can be observed, therefore goes beyond a proof of principle. It provides an evaluation of the practical utility of an algorithmic foundation that supports future quantum applications.

1.3 Characteristics of QFT

QFT includes many controlled-phase rotation gates and two-qubit gate operations. As the number of qubits increases, circuit complexity grows, and the effects of small-angle controlled-phase rotation gates, operations between non-neighboring qubits, compilation efficiency, gate error rates, and error accumulation become more visible in execution results.

1.4 Exact QFT and Approximate QFT

Exact QFT is an exact implementation of the Fourier transform that preserves the quantum state and can be used as an internal subroutine that passes the state to subsequent quantum operations. However, as the number of qubits increases, circuit complexity grows, and execution on the Helios system becomes more susceptible to error accumulation.

Approximate QFT suppresses circuit complexity by omitting small-angle controlled-phase rotation gates. Although the approximation introduces theoretical error, in an experimental environment dominated by error accumulation, the benefit of reducing the gate count can outweigh the approximation error and may produce a higher P_{target} than exact QFT[3].

1.5 Experimental Evaluation

In this paper, we conducted an experimental evaluation of exact QFT and Approximate QFT on both physical and logical qubits using Helios®, Quantinuum's trapped-ion quantum computer.

2. Experimental Evaluation of QFT on Physical Qubits

2.1 Exact QFT with n = 3, 4, and 8 Physical Qubits

As a starting point for evaluating QFT on physical qubits, we used Quantinuum's trapped-ion quantum computer Helios® to examine the target-state probability P_{target} obtained from circuits with relatively small qubit counts (n = 3, 4, and 8). Here, P_{target} denotes the fraction of measurements on the Helios system in which the target output expected from the ideal circuit was observed. For the three target output states (see Figure 2), P_{target} was 0.996–1.000 for n = 3, 0.994–0.996 for n = 4, and 0.976–0.986 for n = 8, showing high P_{target} values in the small-qubit-count regime.

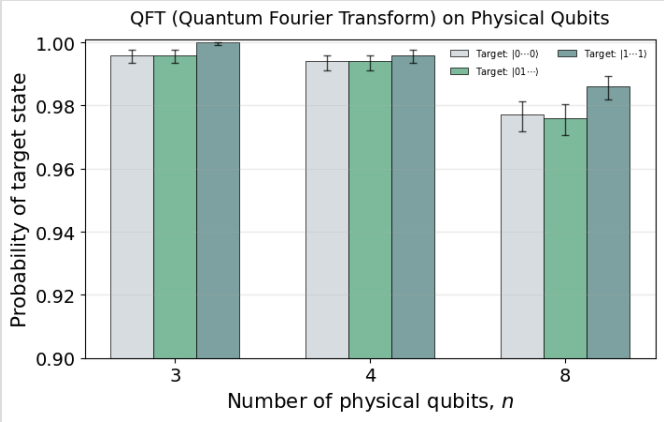

Figure 2. State-by-state P_{target} in exact QFT (n = 3, 4, and 8 physical qubits; shots: 1,000)

2.2 Approximate QFT: Omitting Small-Angle Controlled-Phase Rotation Gates

As the number of qubits increases and the circuit becomes more complex, errors accumulate on the Helios system, making P_{target} more likely to decrease. Therefore, this evaluation used Approximate QFT, which reduces circuit complexity by omitting small-angle controlled-phase rotation gates (see Figure 3).

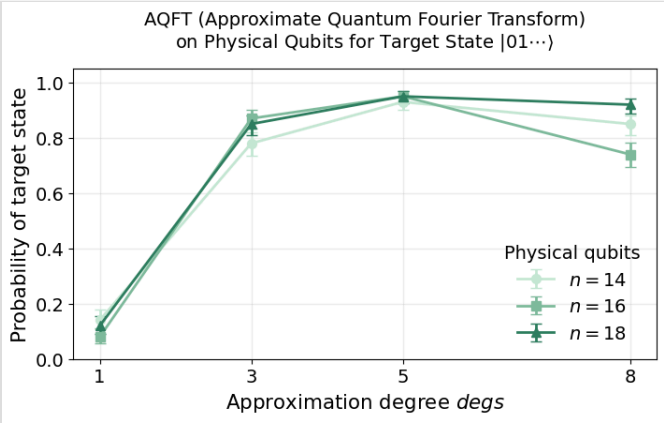

Figure 3. Relationship between approximation degree (degs) and P_{target} in Approximate QFT (n = 14, 16, and 18 physical qubits; shots: 100)

We varied the approximation-degree parameter (degs), which determines how far small-angle controlled-phase rotation gates are omitted. The comparison showed that, in this evaluation, setting this parameter to 5 provided a favorable balance between the theoretical approximation error and the decrease in P_{target} caused by errors on the Helios system.

2.3 Scaling Evaluation of Approximate QFT (up to 98 Physical Qubits)

With the approximation-degree parameter (degs) set to 5, we expanded the number of physical qubits up to 98 and evaluated the scaling behavior of Approximate QFT. In this evaluation, we applied leakage detection (LD), using the ion-state transition-error measurement functionality provided on the Helios system, and measured P_{target} over accepted shots after post-selection. P_{target} was 0.976, 0.904, 0.548, 0.400, and 0.143 for 18, 28, 56, 78, and 98 physical qubits, respectively, with a clear decrease from 56 physical qubits onward due to error accumulation (see Figure 4).

LD-based post-selection improved P_{target} over accepted shots relative to the baseline, while the acceptance rate decreased markedly as the number of qubits increased. When scaling by increasing only the number of physical qubits, the decrease in P_{target} and the decline in acceptance rate progressed simultaneously. In particular, from 78 physical qubits onward, the improvement provided by LD functionality itself also became smaller, suggesting scalability challenges for an approach based only on physical qubits.

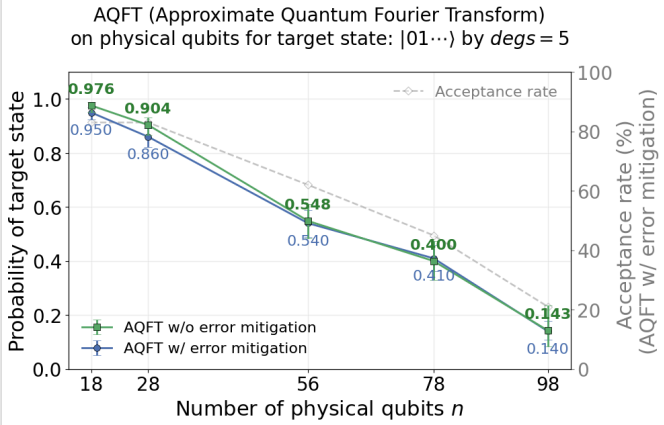

Figure 4. P_{target} and acceptance rate in the scaling evaluation of Approximate QFT (up to 98 physical qubits; including LD functionality; shots: 100)

3. QFT on Logical Qubits

Encoding into logical qubits is a promising way to suppress the impact of physical errors in a quantum computer. At the same time, implementing the non-Clifford logical operations required for QFT in a fault-tolerant manner introduces overhead from additional encoding, verification, measurement, and classical feedforward. This section evaluates QFT on logical qubits on the Helios system from two perspectives: (i) the levels of logical target-state probability $P^{\mathrm{L}}_{\mathrm{target}}$ and acceptance rate achieved through logical-qubit encoding, and (ii) how the choice of implementation method for non-Clifford logical operations affects $P^{\mathrm{L}}_{\mathrm{target}}$ and the acceptance rate.

3.1 Logical-qubit construction using the Steane code

The Steane code is a distance-3 quantum error-correcting code that encodes one logical qubit into seven physical qubits, enabling detection and correction of a single physical-qubit error. It also supports Clifford operations as transversal operations, in which the same operation is applied in parallel to each physical qubit, making it one suitable code for evaluating logical circuits.

3.2 Implementation methods for non-Clifford logical operations

For implementation methods of non-Clifford logical operations, we compare **the direct analog rotation method (Direct Analog Rotation (Non-FT))** and **the code-switching injection method (Code-Switching + Injection (FT))**, based on the amount of added protection and circuit overhead (see Figure 5). The former can be applied directly to a logical qubit[4], whereas the latter includes more protective mechanisms: a quantum Reed-Muller (qRM) code resource, a Steane ancilla block, a Steane data block, measurement, and conditional Z/S gate correction[5][6].

Table 1. Comparison of implementation methods for non-Clifford logical operations

Method	Configuration and overhead
(1) Direct analog rotation method	One Steane data block. The implementation uses 8 physical qubits and does not involve mid-circuit measurement or feedforward correction.
(2) Code-switching injection method	One qRM resource block, one Steane ancilla block, and one Steane data block. The implementation uses 30 physical qubits and includes a transversal T gate on qRM, Code-Switching, and conditional Z/S gate correction.

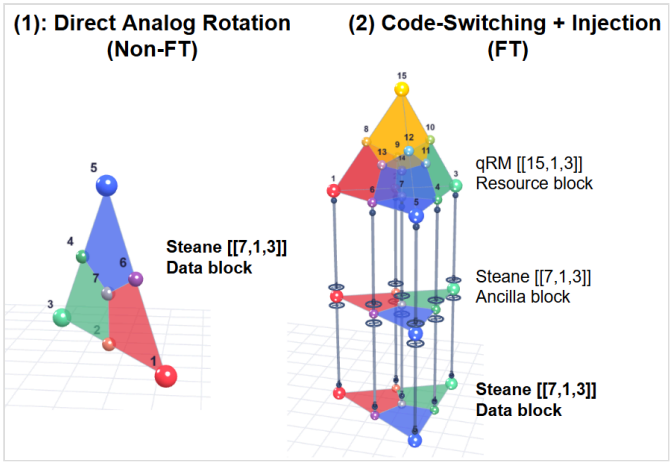

Figure 5. Schematic of implementation methods for non-Clifford logical operations. The left panel shows the direct analog rotation method, and the right panel shows the code-switching injection method. The right panel uses a qRM resource block, a Steane ancilla block, and a Steane data block.

In this comparison, the code-switching injection method includes more protective mechanisms and auxiliary blocks than the direct analog rotation method.

3.3 QFT on logical qubits

QFT on logical qubits has been reported as a target of experimental evaluation on a trapped-ion quantum computer[7]. We evaluate the QFT results based on the direct analog rotation method in terms of $P^{\mathrm{L}}_{\mathrm{target}}$ and the acceptance rate.

Here, we use the logical target-state probability $P^{\mathrm{L}}_{\mathrm{target}}$, defined in Section 2, as the evaluation metric. This is not a quantity defined as the overlap between quantum states; rather, it represents the fraction of decoded or extracted measurement outcomes in which the target output expected from the ideal logical circuit was observed. The **acceptance rate** refers to the fraction of shots that passed conditions such as error-detection post-selection and remained in the final analysis.

In this evaluation, we use three extraction methods for the measurement results: (i) the direct readout method, which evaluates logical values from physical bit strings without error detection or error correction; (ii) the error-detection post-selection method, which excludes shots that may contain errors; and (iii) the error-correction method, which corrects physical-bit errors based on detected-error information.

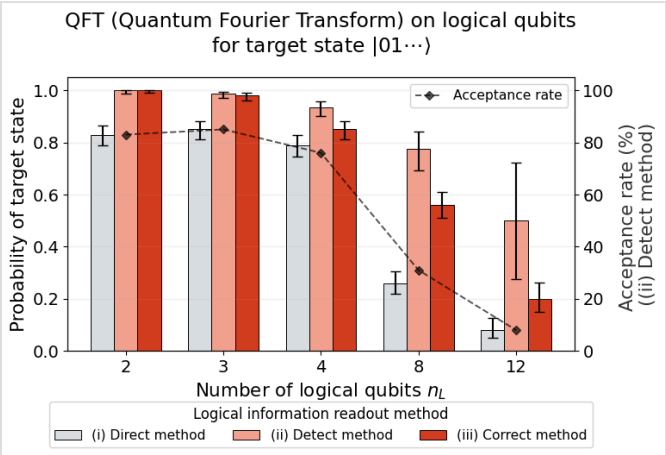

Figure 6. P^{L}_{target} and acceptance rate for QFT based on the direct analog rotation method (Steane code; 100 shots, except 50 shots for n_L = 12)

For QFT on logical qubits, error-detection post-selection improved P^{L}_{target}. In particular, the error-detection post-selection method achieved P^{L}_{target} values of 1.000, 0.988, and 0.934 for n_L = 2, 3, 4, respectively, exceeding the direct readout method. The error-correction method also showed improvement without discarding shots.

At the same time, as the number of logical qubits increases, the reduction in acceptance rate caused by post-selection becomes more pronounced. For n_L = 8, P^{L}_{target} after method (ii), error-detection post-selection, improved to 0.774, but the acceptance rate fell to 31%. For n_L = 12, the acceptance rate further decreased to 8%, so the limited number of accepted shots must be considered when estimating P^{L}_{target}.

The Steane code can correct up to one physical error and detect up to two physical errors. Error correction is therefore effective when single errors are dominant; however, if two or more errors or correlated errors are present, the decoder may incorrectly treat them as a single error and apply an erroneous correction. Because the error-detection post-selection method discards shots in which such errors are suggested, it can improve P^{L}_{target} relative to the error-correction method, at the cost of a lower acceptance rate.

3.4 Comparison of direct analog rotation and code-switching injection for two-logical-qubit QFT

In the comparison of implementation methods for two logical qubits, we compare the direct analog rotation method and the code-switching injection method for non-Clifford operations on logical qubits. The comparison metric is the fraction of accepted shots in which the expected output $|01\rangle$ was observed, namely P^{L}_{target} over accepted shots.

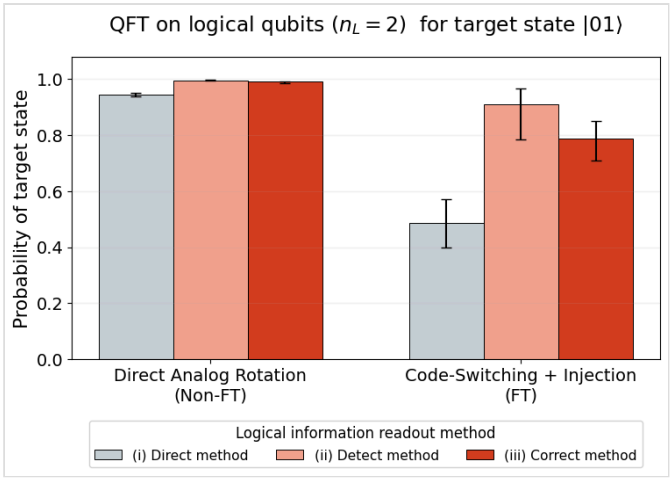

Figure 7. P^{L}_{target} and acceptance rate for direct analog rotation and code-switching injection in two-logical-qubit QFT (shots: 1,000 for direct analog rotation; 100 for code-switching injection)

For the direct analog rotation method, P^{L}_{target} values of 0.945, 0.996, and 0.990 were obtained for (i) direct readout, (ii) error-detection post-selection, and (iii) error correction, respectively (see Figure 7). By contrast, the code-switching injection method yielded 0.485, 0.909, and 0.788 for methods (i), (ii), and (iii), respectively, and was below the direct analog rotation method for all extraction methods. Under the conditions of this evaluation, the additional protective mechanisms incorporated into the code-switching injection method, such as the qRM resource, ancilla block, and conditional correction, did not lead to an advantage in P^{L}_{target}. However, recent theoretical work has advanced low-overhead FT logical gates based on code switching, and the development of implementation methods with FT properties, including the code-switching injection method, remains important for realizing FTQC[8].

4. Conclusion and Outlook

Mitsui & Co., Ltd. and Mitsubishi Electric Corporation evaluated QFT, a foundational quantum algorithm for quantum applications across various fields, on Quantinuum's trapped-ion quantum computer, Helios®.

For physical qubits, Approximate QFT was executed with up to 98 physical qubits. In the small-qubit regime (n = 3, 4, and 8), P_{target} remained high, but it declined from 56 qubits onward and reached 0.143 at 98 qubits. Under the conditions of this evaluation, these results suggest that scaling QFT on physical qubits is limited by accumulated errors, making the need for error correction more apparent as scale increases.

For logical qubits, QFT was executed with up to 12 logical qubits using the Steane code. Under the conditions of this evaluation, error-detection post-selection was suggested to yield $P^{\text{L}}_{\text{target}}$ comparable to or higher than that obtained with error correction. However, within the range confirmed in this evaluation, the acceptance rate decreased from 83% to 8% as the number of logical qubits increased, indicating a trade-off between $P^{\text{L}}_{\text{target}}$ and the acceptance rate.

In the comparison of non-Clifford logical operations for two-logical-qubit QFT, both the direct analog rotation method and the code-switching injection method ran on the Helios system. At the scale evaluated here, however, the direct analog rotation method (Non-FT) showed higher $P^{\text{L}}_{\text{target}}$. For realizing FTQC, continued development of implementation methods with fault-tolerant properties, including the code-switching injection method, remains important.

These findings indicate that the transition toward FTQC requires cross-layer design spanning the algorithm layer (including the design of approximation degree), the error-correction layer (including quantum error-correcting codes), and the hardware layer (including the use of all-to-all qubit connectivity).

Future Outlook and Challenges

When extending these findings to quantum applications such as cryptanalysis, quantum chemistry, and financial simulation, it will be necessary to estimate the resources required for implementation on actual quantum hardware, including circuit complexity, overhead, and shot counts, and to define concrete implementation strategies. Evaluation methods should also be organized and extended so that resource metrics can be incorporated alongside quality metrics such as P_{target}, $P^{\text{L}}_{\text{target}}$ and the acceptance rate.

Quantum-Related Initiatives

[Mitsubishi Electric Corporation]
Mitsubishi Electric Corporation promotes research and development in quantum computing, quantum communication and security, quantum sensing, and quantum devices. In particular, it is pursuing practical initiatives such as control technologies for connecting multiple quantum devices, post-quantum cryptography (PQC), and quantum AI applications.

[Mitsui & Co., Ltd.]
Through its equity investment in and sales partnership with Quantinuum, Mitsui & Co., Ltd. is expanding its quantum technology business with a focus on Japan and the Asia-Pacific region. In parallel, Mitsui & Co., Ltd. is also engaged in the development and validation of specific use cases, including quantum cybersecurity and quantum applications for drug discovery and materials development.

Notes

These notes supplement the key technical terms used in this paper.

QFT / exact QFT / Approximate QFT
QFT stands for Quantum Fourier Transform. Exact QFT refers to an implementation that includes all controlled-phase rotations in the ideal QFT circuit. Approximate QFT omits some small-angle controlled-phase rotation gates to reduce circuit complexity.

QFT on physical qubits / QFT on logical qubits
This paper distinguishes QFT or Approximate QFT executed on physical qubits from QFT executed on logical qubits encoded with a quantum error-correcting code. The main metrics are the target-state probability P_{target} in the former case, and the logical target-state probability $P^{\mathrm{L}}_{\mathrm{target}}$ and acceptance rate in the latter case.

Partial-FTQC / FTQC
Partial-FTQC refers to an intermediate stage toward full fault-tolerant quantum computing that uses limited error detection, error correction, and logical encoding. FTQC stands for Fault-Tolerant Quantum Computing.

QCCD
QCCD stands for Quantum Charge-Coupled Device. It is an architecture for trapped-ion quantum computers in which ions are moved and rearranged as they are supplied to operation zones.

All-to-all connectivity
Connectivity that allows two-qubit gates to be executed between arbitrary pairs of qubits.

Acceptance rate / number of accepted shots
The acceptance rate is the fraction of shots that pass conditions such as error-detection post-selection and remain in the final analysis. The number of accepted shots is reported together with the total number of shots.

Leakage detection (LD)
A method for detecting quantum states that have leaked out of the computational basis space and excluding the corresponding shots based on the detection result. In this paper, LD is used as a post-selection method in evaluations of QFT / Approximate QFT on physical qubits, using the ion transition-error measurement functionality provided on the Helios system.

Steane code
A distance-3 quantum error-correcting code that encodes one logical qubit using seven physical qubits. This paper uses it to evaluate QFT on logical qubits.

Transversal operation
A way to implement a logical gate by applying physical gates of the same form in parallel to the physical qubits that make up a logical qubit. It has the advantage of making errors less likely to spread within a code block.

Quantum Reed-Muller (qRM) code
A code from the quantum Reed-Muller family. This paper discusses it in relation to the code-switching injection method in the context of non-Clifford logical operations and state injection.

Non-Clifford operation
Because Clifford operations alone are not sufficient for universal quantum computation, non-Clifford operations such as T gates are required.

Direct analog rotation method
A non-Clifford operation implementation for Partial-FTQC that combines error-corrected Clifford operations with analog rotations. In this paper, it is treated as the lower-overhead implementation scheme compared with the code-switching injection method.

Code switching
A method that converts a logical state between different quantum error-correcting codes and uses the logical operations suited to each code. In this paper, code switching is treated as an element of the code-switching injection method: it exploits the fact that a transversal T gate cannot be used directly in the Steane code but can be used in the qRM code, enabling non-Clifford operations such as T gates.

Conditional Z/S gate correction
A correction operation equivalent to a Z gate or S gate that is applied depending on the measurement result or code-switching result. In the code-switching injection method, it is treated as a feedforward operation that aligns the logical state to the desired frame after resource-state injection.

References

[1] Babbush et al., “Securing Elliptic Curve Cryptocurrencies against Quantum Vulnerabilities: Resource Estimates and Mitigations,” arXiv:2603.28846v2, 2026. https://arxiv.org/abs/2603.28846

[2] Quantinuum, “Quantinuum Helios Product Data Sheet,” Version 1.01, January 21, 2026. https://docs.quantinuum.com/systems/data_sheets/Quantinuum%20Helios%20Product%20Data%20Sheet.pdf

[3] D. Coppersmith, “An Approximate Fourier Transform Useful in Quantum Factoring,” IBM Research Report RC 19642, 1994; arXiv:quant-ph/0201067.

[4] Akahoshi et al., “Partially Fault-Tolerant Quantum Computing Architecture with Error-Corrected Clifford Gates and Space-Time Efficient Analog Rotations,” *PRX Quantum* **5**, 010337, 2024. https://doi.org/10.1103/PRXQuantum.5.010337

[5] Daguerre et al., “Experimental demonstration of high-fidelity logical magic states from code switching,” *Physical Review X* **15**, 041008, 2025. https://doi.org/10.1103/dck4-x9c2

[6] Anderson et al., “Fault-tolerant conversion between the Steane and Reed-Muller quantum codes,” *Physical Review Letters* **113**, 080501, 2014. https://doi.org/10.1103/PhysRevLett.113.080501

[7] Mayer et al., “Benchmarking logical three-qubit quantum Fourier transform encoded in the Steane code on a trapped-ion quantum computer,” arXiv:2404.08616, 2024. https://arxiv.org/abs/2404.08616

[8] L. Golowich, K. Chang, and G. Zhu, “Constant-Overhead Addressable Gates via Single-Shot Code Switching,” arXiv:2510.06760, 2025. https://arxiv.org/abs/2510.06760

Copyright and Reproduction

Disclaimer